AFRL-RH-WP-TR-2012-0130

Development of a 2,4-Dinitrotoluene-Responsive Synthetic Riboswitch in *E. coli* cells

Molly E. Davidson
UES, Inc.
4401 Dayton-Xenia Road
Dayton OH 45432

Svetlana V. Harbaugh
Yaroslav G. Chushak
The Henry M. Jackson Foundation
6720A Rockledge Drive
Bethesda MD 20817

Morley O. Stone
Nancy Kelley-Loughnane
Human Signatures Branch
2800 Q Street
Wright-Patterson AFB OH 45433

SEPTEMBER 2012

Final Report

AIR FORCE RESEARCH LABORATORY
711TH HUMAN PERFORMANCE WING,
HUMAN EFFECTIVENESS DIRECTORATE,
WRIGHT-PATTERSON AIR FORCE BASE, OH 45433
AIR FORCE MATERIEL COMMAND
UNITED STATES AIR FORCE

NOTICE AND SIGNATURE PAGE

This report was cleared for public release by the 88th Air Base Wing Public Affairs Office and is available to the general public, including foreign nationals. Copies may be obtained from the Defense Technical Information Center (DTIC) (http://www.dtic.mil).

AFRL-RH-WP-TR-2012-0130 HAS BEEN REVIEWED AND IS APPROVED
FOR PUBLICATION IN ACCORDANCE WITH ASSIGNED DISTRIBUTION STATEMENT.

//signature//

Nancy Kelley-Loughnane Work Unit Manager
Human Signatures Branch

//signature//

Louise A. Carter, Chief
Forecasting Division
Human Effectiveness Directorate
711th Human Performance Wing
Air Force Research Laboratory

REPORT DOCUMENTATION PAGE

Form Approved
OMB No. 0704-0188

1. REPORT DATE *(DD-MM-YY)*	2. REPORT TYPE	3. DATES COVERED *(From - To)*
01 09 12	Final	Feb 19, 2008 – Sep 1, 2012

4. TITLE AND SUBTITLE

Development of a 2,4-Dinitrotoluene-Responsive Synthetic Riboswitch in *E. coli* cells

5a. CONTRACT NUMBER
IN-HOUSE

5b. GRANT NUMBER

5c. PROGRAM ELEMENT NUMBER
0601102F

6. AUTHOR(S)
Molly E. Davidson[†], Svetlana V. Harbaugh[‡*], Yaroslav G. Chushak[‡], Morley O. Stone, Nancy Kelley-Loughnane[*]

5d. PROJECT NUMBER
2312

5e. TASK NUMBER
A

5f. WORK UNIT NUMBER
H04J (2312A217)

7. PERFORMING ORGANIZATION NAME(S) AND ADDRESS(ES)
[†]UES, Inc.
4401 Dayton-Xenia Road
Dayton, OH 45432

[‡]The Henry M Jackson Foundation
6720A Rockledge Drive
Bethesda MD 20817

8. PERFORMING ORGANIZATION REPORT NUMBER

9. SPONSORING/MONITORING AGENCY NAME(S) AND ADDRESS(ES)
Air Force Materiel Command
Air Force Research Laboratory
711th Human Performance Wing
Human Effectiveness Directorate
Forecasting Division
Human Signatures Branch
Wright-Patterson Air Force Base, OH 45433

10. SPONSORING/MONITORING AGENCY ACRONYM(S)
711 HPW/RHXB

11. SPONSORING/MONITORING AGENCY REPORT NUMBER(S)
AFRL-RH-WP-TR-2012-0130

12. DISTRIBUTION/AVAILABILITY STATEMENT
Distribution A: Approved for public release; distribution is unlimited.

13. SUPPLEMENTARY NOTES
88ABW-2012-5366, cleared on 10 Oct 2012

14. ABSTRACT

Riboswitches are RNA sequences that regulate expression of associated downstream genes in response to the presence or absence of specific small molecules. A novel riboswitch that activates protein translation in *E. coli* cells in response to 2,4-dinitrotoluene (DNT) has been engineered. A plasmid library was constructed by incorporation of 30 degenerate bases between a previously described trinitrotoluene aptamer and the ribosome binding site. Screening was performed by placing the riboswitch library upstream of the Tobacco Etch Virus (TEV) protease coding sequence in one plasmid; a second plasmid encoded a FRET-based construct linked with a peptide containing the TEV protease cleavage site. Addition of DNT to bacterial culture activated the riboswitch, initiating translation of TEV protease. In turn, the protease cleaved the linker in the FRET-based fusion protein, causing a change in fluorescence. This new riboswitch exhibited a 10-fold increase in fluorescence in the presence of 0.5 mM DNT compared to the system without target.

15. SUBJECT TERMS
Riboswitch, Dinitrotoluene, Trinitrotoluene, FRET, TEV protease, REACh

16. SECURITY CLASSIFICATION OF:			17. LIMITATION OF ABSTRACT:	18. NUMBER OF PAGES	19a. NAME OF RESPONSIBLE PERSON (Monitor)
a. REPORT	b. ABSTRACT	c. THIS PAGE			Nancy Kelley-Loughnane
U	U	U	SAR	37	19b. TELEPHONE NUMBER *(Include Area Code)* N/A

Standard Form 298 (Rev. 8-98)
Prescribed by ANSI Std. Z39-18

THIS PAGE IS INTENTIONALLY LEFT BLANK

TABLE OF CONTENTS

LIST OF FIGURES

1.0 INTRODUCTION

Riboswitches are naturally-occurring genetic regulatory elements found in the 5′ untranslated region of some mRNA. They provide a method for cellular response to the presence or absence of metabolites by regulating the translation of downstream genes. Numerous examples of naturally occurring bacterial riboswitches have been discovered (reviewed in ref. 1). The size and structure of metabolite targets vary significantly, an indication that riboswitches could be used to detect a wide range of targets[2]. This apparent versatility of riboswitches in nature is being exploited by researchers in order to develop synthetic riboswitches that regulate gene expression in response to desired target molecules. The advantage of such engineered riboswitches is that they offer a way to control gene expression via non-natural molecules, e.g. drug compounds.

Riboswitch-containing cells are appealing as sensors because they are self-replicating and have the potential to sense a target for an extended period of time, over the life of the cell culture. In many instances, it may be easier to preserve bacterial cell function than to preserve antibody structure or enzymatic activity for sensing purposes. For example, antibodies are highly sensitive to pH, temperature changes, and variation in salt concentration. Bacteria, however, is more tolerant and, in addition, can be protected from environmental conditions as a way of hardening the sensor system to increase operational lifetime, improve portability, and preserve function of cells[3-6].

Riboswitches are composed of two functional elements: a biological recognition element (aptamer), and an expression platform. The aptamer binds specifically to a small-molecule target and changes conformation in response to the binding event. The resulting conformational change can cause up- or down-regulation of translation of downstream genes based on the availability of the ribosome binding site. For sensing applications riboswitch activation should produce a positive signal

when the aptamer binds the target. Ideally, the increase in signal intensity will be proportional to the amount of target detected by the system, as this provides a mechanism for quantification of the target.

Aptamers that recognize specific target molecules have been selected using techniques such as Systematic Evolution of Ligands by EXponential Enrichment (SELEX)[7] and allosteric selection[8]. Linking a specifically selected aptamer with an expression platform may yield a novel riboswitch that is active in cells and could be used to detect a molecule of interest[2, 9, 10].

Recently, Ehrentreich-Forster and colleagues selected and tested 2,4,6-trinitrotoluene (TNT)-specific aptamer for use in explosives sensing devices[11]. They developed a method for detection of TNT utilizing a flow cell with immobilized TNT and fluorescently labeled aptamer that exhibited a decrease in fluorescent signal when TNT was present in the sample. We coupled this aptamer with a partially randomized expression platform to develop a riboswitch for the detection of TNT structural analog, 2,4-dinitrotoluene (DNT). DNT differs from TNT in that it lacks the presence of a third nitro group. We assumed that the lack of the third nitro group will not have a drastic affect on the binding ability of DNT to the aptamer.

2,4-Dinitrotoluene is an explosive chemical that is used in the production of the polyurethane foam for bedding and furniture industries and as a gelating agent in explosives, ammunition, and dyes[12]. The detection of DNT is important for a few reasons. First, from a security perspective, DNT is an intermediate in the production of TNT, the most commonly used explosive in the world, and is released in the effluent following TNT manufacturing. The presence of DNT (concentration range of 0.04-48.6 mg/L) was detected with 100% of occurrence rate in wastewater samples (n = 54) collected from the effluent pipe of TNT production facility[13].

Detection of DNT in a location could be an indicator of terrorist activity. Second, DNT from industrial waste can remain in soil and bodies of water for extended periods of time, posing a risk for humans and animals that are exposed. The toxic effects of DNT have been observed in bacteria, fish, reptiles

and other animals which act as indicators of toxicity in humans[12, 14-17]. Dangers associated with DNT exposure include immunosuppression, smooth muscle cell damage, and circulatory and cardiovascular problems[18].

This article describes the development of a synthetic riboswitch in *E. coli* cells that enables detection of DNT. An aptamer selected to bind TNT molecules[11] was linked with a PCR-generated expression platform library placed upstream of the gene encoding Tobacco Etch Virus (TEV) protease. The riboswitch sensor output is based on the principle of Fluorescence Resonance Energy Transfer (FRET). Briefly, enhanced green fluorescent protein (eGFP) was linked to a non-fluorescent mutant yellow fluorescent protein called REACh (Resonance Energy Accepting Chromoprotein) [19]. Use of this type of FRET pair eliminates acceptor fluorescence, therefore little to no fluorescence is observed prior to cleavage[20]. The linker between these two proteins contains the TEV protease cleavage site. Upon activation of the riboswitch, TEV protease is translated and cleaves the FRET linker, allowing the detection of eGFP fluorescence. The selected riboswitch exhibited a 10-fold increase in fluorescence in the presence of 0.5 mM DNT compared to the system without target.

2.0 MATERIALS AND METHODS

2.1 Materials

Ampicillin, chloramphenicol, dimethyl sulfoxide, rhamnose, 4-nitrophenol (4-NP), and 2,4-dinitrotoluene were purchased from Sigma Chemical Company (St. Louis, MO). PCR primers were obtained from MWG Operon (Huntsville, AL). Phusion DNA polymerase was purchased from New England BioLabs (Ipswich, MA). Difco LB was purchased from Becton, Dickinson and Company (Franklin Lakes, NJ). TOP10 competent *E. coli* were purchased from Invitrogen (Carlsbad, CA). The tobacco etch virus protease gene construct and plasmid pHWG640 were generous gifts from Dr. Hele-

na Berglund from Karolinska Institute, Stockholm, Sweden and Dr. Josef Altenbuchner from the Institute of Industrial Genetics at the University of Stuttgart, Germany, respectively. The plasmid pSAL8.1 was kindly provided by Dr. Justin Gallivan from Emory University, Atlanta, GA. Trinitrotoluene DNA aptamer sequence upstream of TEV protease coding sequence was purchased from DNA 2.0 (Menlo Park, CA).

Plasmid manipulations were performed using chemically competent MAX Efficiency DH5α *E. coli* cells. Full descriptions of primer sequences and plasmid construction techniques are available in the Supplemental Information.

2.2 Construction of the plasmid library

PCR primers were designed to provide incorporation of up to 30 degenerate bases between the TNT aptamer[11] and the Shine-Dalgarno sequence (ribosome binding site)[21]. PCR was performed in order to insert the randomized expression platform into the pSAL:TNTaptTEV construct. The resulting plasmid library and pHWG640:eGFP-TL-REACh were transformed into *E. coli* TOP10 cells and cells were grown overnight at 37°C.

2.3 Screening of riboswitch clones

Each of the riboswitch clones was screened on LB agar plates with and without 0.5 mM DNT. Colonies showing high fluorescence were selected for screening in aqueous medium. Briefly, 24-well plates containing 1 mL/well LB medium, supplemented with ampicillin (100 µg/mL) and chloramphenicol (25 µg/mL), were seeded with 20 µL overnight culture. Cultures were grown for 2.5 hrs at 37°C, 220 rpm. Rhamnose was added to each well to a final concentration of 0.4%. Thirty minutes after addition of rhamnose, 2,4-DNT was added to "ON" cultures to a final concentration of 0.5 mM. An equivalent volume of DMSO was added to "OFF" cultures. Absorbance at 600 nm and fluorescence at 510 nm (excitation 457 nm) were measured immediately after addition of DNT, and 6 hours

later. The activation ratio of each culture was determined by dividing the normalized fluorescence of the "ON" state at 6 hours by the normalized fluorescence of the "OFF" state at 6 hours.

2.4 Time course experiments

For time course studies, pHWG640:eGFP-TL-REACh and a TEV protease expressing plasmid, either pSAL:TEV, pSAL:RS2A-2TEV, or pSAL:RS2A-2TEVC151A, were transformed into chemically competent *E. coli* TOP10 cells. Three separate colonies of *E. coli* TOP10 cells harboring either the positive control (pHWG640:eGFP-TL-REACh and pSAL:TEV), riboswitch (pHWG640:eGFP-TL-REACh and pSAL:RS2A-2TEV), or negative control (pHWG640:eGFP-TL-REACh and pSAL:RS2A-2TEVC151A) were picked from LB agar plates containing ampicillin (100 µg/mL) and chloramphenicol (25 µg/mL) and grown overnight at 37°C in separate flasks containing 50 mL of LB media supplemented with ampicillin (100 µg/mL) and chloramphenicol (25 µg/mL). A 1.5 mL aliquot of the overnight cultures was used to inoculate 150 mL of LB supplemented with ampicillin (100 µg/mL) and chloramphenicol (25 µg/mL). Cultures were grown at 37°C to an OD_{600} of 0.4-0.5 and induced with 0.4% rhamnose for pHWG640:eGFP-TL-REACh expression. Thirty minutes after induction, cultures harboring positive control, riboswitch, or negative control were treated with 0.5 mM DNT in DMSO, or equivalent volume of DMSO for riboswitch in "OFF" state. OD_{600} of each culture and fluorescence at 510 nm (excitation 457 nm) were measured at time 0 (when DNT or vehicle was added), 1, 2, 3, 4, 5, and 6 hours after riboswitch activation. At each time point, 10 mL of culture was collected for cell lysis, protein determination, and fluorescence readings. Cell pellets were stored at -80°C until ready for processing. Cell pellets were resuspended in 0.4 mL lysis buffer (100 mM Tris-HCl, pH 8.0, 150 mM NaCl, 1 mM $MgCl_2$) and incubated on ice for 30 minutes. The buffer was supplemented with lysozyme (0.1mg/mL), Benzonase® Nuclease (10 µL/10 mL) and iodoacetamide (8 mM). Cell debris was removed by centrifugation at 14000 x g for 30 minutes at 4°C in an Eppendorf 5417R centrifuge

(Fisher Scientific, Pittsburgh, PA). Protein concentrations of the clarified cellular extracts were determined by BCA assay; fluorescence at 510 nm was read, as described above. Riboswitch negative control experiments were performed exactly as above, substituting DNT with 4-nitrophenol at a concentration of 0.1 mM. All time course studies were conducted in triplicate, and data are presented as the mean ± s.e.m.

2.5 Dose response experiments

Dose response experiments were performed as described above for time course experiments. DNT was added to the media at various concentrations (0.005, 0.01, 0.05, 0.1, 0.25, and 0.5 mM) and cells were harvested and lysed at time 6 hours. Total protein concentrations, fluorescence and OD_{600} were determined as described above.

2.6 Analysis of secondary structure of the riboswitch

The secondary structure of the riboswitch was analyzed using enzymatic probing. Cleavage fragment sizes were predicted manually based on the cleavage specificities of RNases A and T1 (Ambion, Austin, TX). Riboswitch RNA was incubated with or without DNT in Structure Buffer for 15 min. at room temperature prior to addition of RNA-grade ribonucleases. Reactions were carried out according to manufacturer's protocol. Dried sample pellets were resuspended in 10 µL of nuclease-free water and denatured at 70°C for 2 min. prior to analysis on a 2100 BioAnalyzer, using the Small RNA Kit (Agilent, Santa Clara, CA). Peak sizes obtained experimentally were compared to relative likelihood of fragment size occurrence as determined by cleavage analysis of secondary structures predicted by Mfold[22] and of the predicted secondary structure provided in Ehrentreich-Förster's publication, which accounts for proximity to TNT[11].

3.0 RESULTS AND DISCUSSION

We used a previously described TNT binding RNA[11] (K_d = 1 X 10^{-8} M) as an aptamer domain to develop a synthetic riboswitch to detect the TNT structural analog, DNT. In order to determine the concentration of analyte suitable for riboswitch selection, and considering the high toxicity of 2,4-dinitrotoluene to prokaryotic, plant, and mammalian cells[23, 24], we tested the effect of different concentrations of DNT on the growth of *E. coli* cells. Concentrations of DNT higher than 1 mM were toxic for *E. coli* cells resulting in complete suppression of cell growth (as shown in Figure SI.1). DNT concentration of 0.5 mM slowed down the growth of cells, however, did not change the growth curve (compared to cells without DNT), and was chosen for riboswitch selection.

Using a polymerase chain reaction, we constructed a riboswitch library by incorporating up to 30 degenerate bases between the TNT aptamer and ribosome binding site (RBS) (Figure 1). The riboswitch library was placed upstream of TEV protease encoding sequence under control of the *tac* promoter and co-transformed (with a plasmid encoding FRET-based TEV protease substrate) into *E. coli* TOP10 cells, yielding 627 riboswitch clones. Our screening assay was based on a previously described system including TEV protease and FRET-based substrate production within the same cell[20]. In the absence of analyte, the translation of TEV protease is suppressed, the FRET-based protein substrate remains uncleaved, and cells do not show significant emission at 510 nm upon excitation at 457 nm. In the presence of analyte, TEV protease is produced and cleaves the substrate resulting in fluorescent protein release, loss of FRET-based quenching, and increase in fluorescence intensity of cells. All clones were visually screened for fluorescence increase in the presence of 0.5 mM DNT on LB agar plates. Colonies that appeared to show increased fluorescence in the presence of DNT were selected for further screening in liquid medium on 24-well plates. Ratios of fluorescent intensities for cell cultures grown in the presence of DNT to those grown without DNT (the "activation ratio") were

utilized to identify functional switches. Of the 213 colonies screened in aqueous medium, five showed activation ratios (AR) of greater than three and were selected for sequencing. Expression platform sequences and activation ratios observed in cell culture are shown in Table SI.1. No homology in the expression platforms was observed, even for switches exhibiting the same activation ratios. Moreover, the length of the expression platforms for these top five switches ranged from 15 to 30 nucleotides.

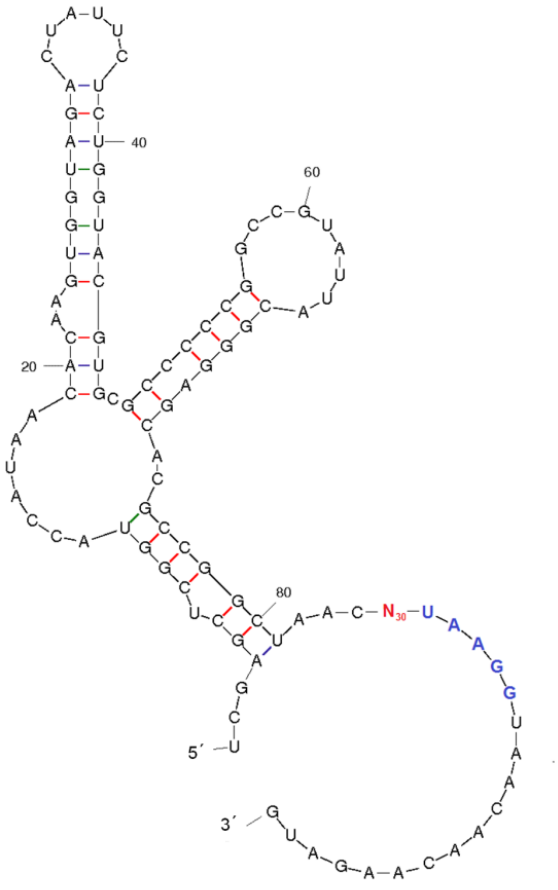

Figure 1. Construction of riboswitch library
Thirty random bases were inserted between the TNT specific aptamer and ribosome binding site (RBS = blue) by PCR. The secondary structure of the TNT aptamer was predicted using Mfold software.

The secondary structure of the selected riboswitches was analyzed using the Mfold package[22]. We calculated the lowest energy structure in "OFF" and "ON" states as well as suboptimal structures. One of the factors that affect an activation rate is an energy barrier or a difference in free energy be-

tween the "OFF" and "ON" state of the riboswitch: if the energy difference between the "OFF" and "ON" states is small, it is very likely that riboswitch can change into an "ON" state even in the absence of ligand. We have found that the riboswitches 2A-2 with the highest activation ratio (AR=9.8) and riboswitch 1B-10 (AR=3.2) have a very similar free energy difference between the "OFF" and "ON" states (ΔG = 5.1 kcal/mol and 4.9 kcal/mol, respectively) as can be seen in Figure 2. On the other hand, riboswitches 1B-10 and 1A-3 have the same activation rate of 3.2 but significantly different energy barrier between the "OFF" and "ON" states, 4.9 kcal/mol and 2.9 kcal/mol, respectively. Therefore, energy barrier alone cannot explain the observed difference in the activation rate of these riboswitches.

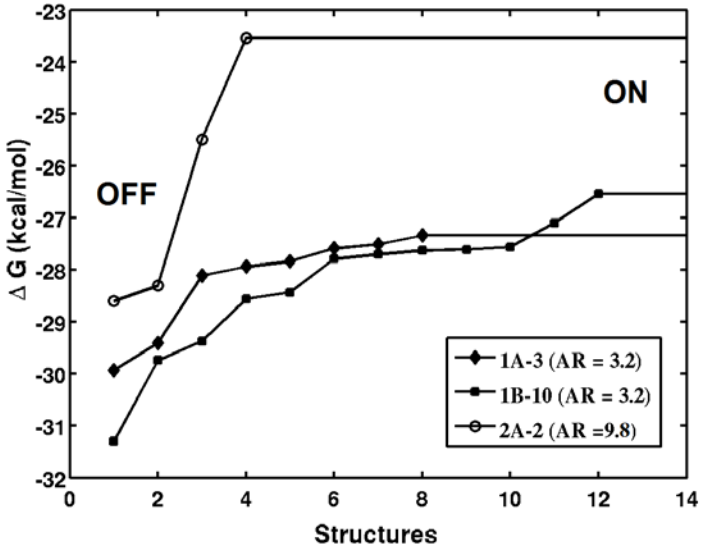

Figure 2. Energy profiles of DNT riboswitches as predicted by Mfold[17]
Riboswitch 2A-2 with the highest activation rate AR=9.8 has a similar energy barrier between the "OFF" and "ON" states as riboswitch 1B-10 with the AR=3.2. However, riboswitch 2A-2 has only two intermediate conformations whereas the riboswitch 1B-10 has 11 intermediate conformations or greater distance between the "OFF" and "ON" states. Riboswitches 1B-10 and 1A-3 have the same activation rate of 3.2 but different energy barriers, 4.9 kcal/mol and 2.9 kcal/mol, respectively.

Next, we analyzed the distance or number of intermediate conformations between the "OFF" and "ON" states of the riboswitches. We found that riboswitch 2A-2 has only two intermediate con-

formations between the "OFF" and "ON" states whereas the riboswitch 1B-10 has 11 intermediate conformations (Figure 2). The existence of many intermediate structures makes it easier for the riboswitch to switch from "OFF" to "ON", thereby lowering the activation rate. This observation is in agreement with results of Hall, Hesselbergth and Ellington[25] who have shown that both the height of the energy barrier and the distance (number of intermediate states) between the active and inactive conformations affect the level of aptazyme activation.

The clone with the highest activation ratio (clone 2A-2; AR= 9.8) was selected for further characterization. In order to validate the selected riboswitch clone, we performed a time course study of riboswitch activation in cell cultures and cell lysates. To confirm the DNT-dependent increase in TEV protease activity, cell cultures harboring the riboswitch construct were compared to control cells harboring TEV protease-encoding sequence without riboswitch and under the control of a constitutive promoter. The fluorescence intensity, measured at the eGFP emission wavelength, 510 nm, increased over time in control and riboswitch cell cultures in the presence of 0.5 mM DNT, and did not show similar changes in the riboswitch cell cultures without analyte (Figure SI.2). We noticed that the riboswitch activation ratio of 2.0, calculated in time course studies was lower than that (9.8) determined in selection experiments. The difference in activation ratios for the same riboswitch construct corresponds with differences in cell growth rates between small and large culture volumes (24-well plate vs. culture flask). The growth curves of control and riboswitch cells with and without analyte were similar (Figure SI.3), demonstrating that 0.5 mM DNT is nontoxic to the cells, and confirming that changes of the spectral profile of these cultures were attributed to riboswitch behavior and do not result from variation in their growth pattern.

We observed a greater riboswitch activation ratio in cell lysates than in cell cultures due to elimination of background fluorescence of the medium. Figure 3 shows the riboswitch activation over time based on the increase in fluorescence intensity at 510 nm. The TEV protease under riboswitch

control displayed a 10-fold increase in signal in the presence of DNT over the riboswitch "OFF" state. The riboswitch "ON" curve was similar to positive control (TEV POS CNTRL) when TEV protease was expressed directly. However, we observed increase in the fluorescence intensity of cell lysates without analyte when riboswitch was in "OFF" state compared to that for the negative control (FRET NEG CNTRL) in which FRET-based protein was produced and accumulated, but not cleaved by TEV protease. The presence of fluorescence background when riboswitch was in "OFF" state indicated the low level of TEV protease expression, even in the absence of analyte, due to riboswitch "leakage" (the inability of the riboswitch to completely maintain the "OFF" state conformation within the cellular system). Surprisingly, the decrease in fluorescence intensity of cells harboring riboswitch without analyte treatment (RS "OFF") occurred at five and six hour time points. In order to show that developed riboswitch can be activated only in the presence of DNT, we treated riboswitch harboring cells with chemical with isomorphic properties to DNT, 4-nitrophenol (riboswitch negative control). 4-nitrophenol was previously used to test the specificity of TNT aptamer[11]. In experiments with 4-nitrophenol, the concentration of analyte was reduced to 0.1 mM due to toxicity of 0.5 mM 4-nitrophenol to the cells (Figure SI.4). The fluorescence profiles of negative control (RS NEG CNTRL) were similar to the profiles of "OFF" state thus indicating the specificity to DNT in newly developed riboswitch (Figure 3).

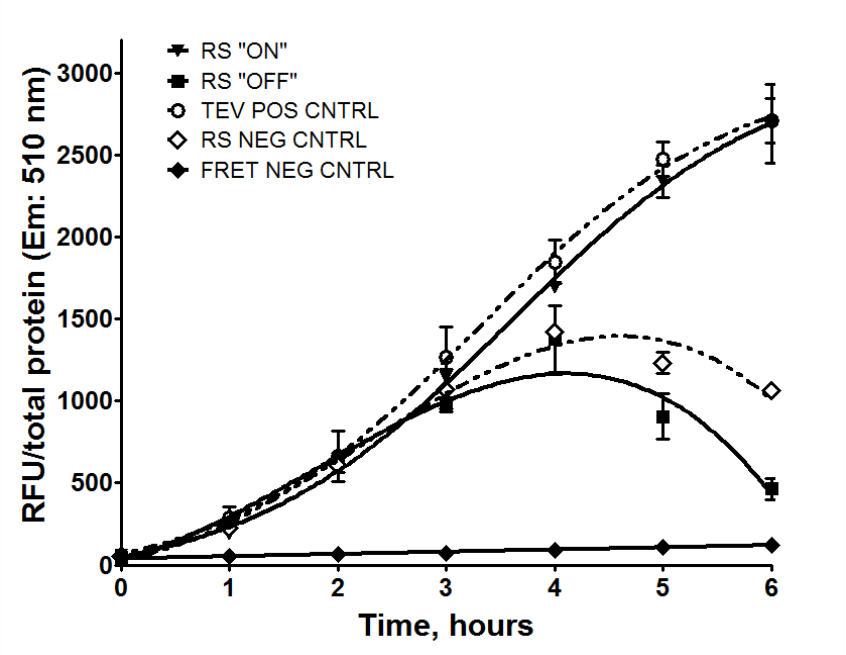

Figure 3. Time course study of riboswitch activation in response to 2,4-dinitrotoluene addition
Emission at 510 nm was monitored in cellular extracts of TOP10 E. coli cells harboring FRET-based protein (TEV protease substrate), eGFP-TL-REACh, and one of the following constructs: TEV protease under control of constitutive promoter (TEV POS CNTRL) (white circles); riboswitch-TEV protease in the presence of DNT (RS "ON") (inverted black triangles); riboswitch-TEV protease (RS "OFF") (black squares); riboswitch TEV protease in the presence of 4-nitrophenol (RS NEG CNTRL) (white rhombus); riboswitch-TEV protease inactive mutant (FRET NEG CNTRL) (black rhombus). 0.5 mM DNT or 0.1 mM 4-nitrophenol was added at time 0, and samples were collected at indicated time points.

We observed a visual difference between riboswitch "OFF" and "ON" states in cellular lysates of harvested cells. Images of cell lysates at indicated time points (Figure 4A) showed a gradual increase in the fluorescence signal of released eGFP due to cleavage of eGFP-TL-REACh by expressed TEV protease in riboswitch activated cells. The cleavage of the FRET-based protein in cellular lysates of riboswitch activated cells was demonstrated by appearance of well-defined eGFP corresponding band in nondenaturing polyacrylamide gel (Figure 4B).

In order to investigate thresholds of the detection, we examined the fluorescence signal in response to varying DNT concentrations. As can be observed in Figure 5, the changes in the fluorescence intensity in response to different analyte concentrations demonstrate a typical dose-response

curve. We were not able to reach a saturation state at higher concentrations of analyte due to the toxic effects of high concentrations of DNT on cell growth and viability. Based on the dose-response curve, the increase in fluorescence intensity can be detected at DNT concentrations as low as 0.05 mM.

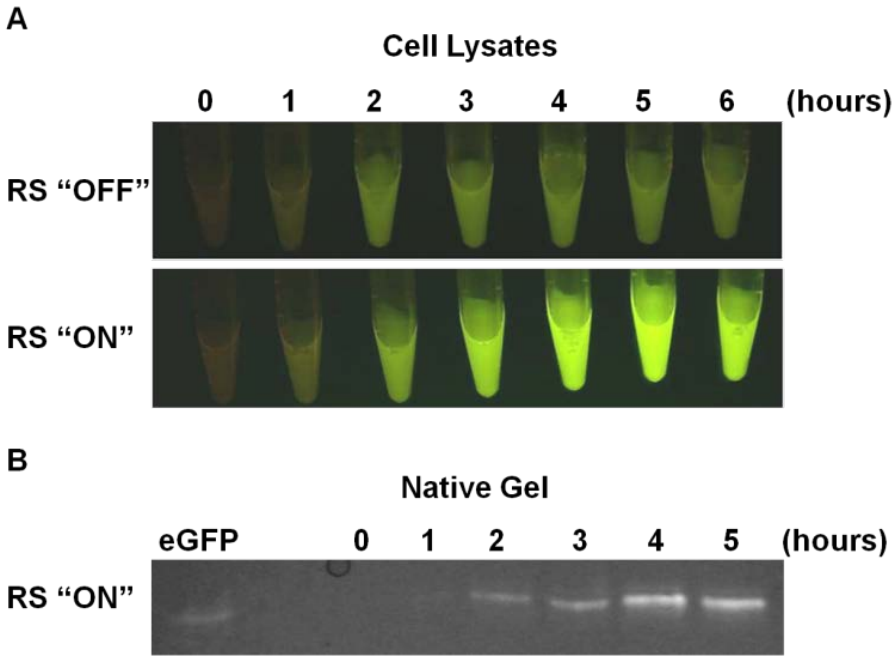

Figure 4. Visualization of DNT dependent riboswitch activation
(A) Images of clarified lysates of cells without DNT treatment (upper panel) and cells exposed to DNT (lower panel) harvested at indicated time points were taken using FUJIFILM digital camera and Dark Reader transilluminator (Clare Chemical Research). (B) 12% Tris-HCl nondenaturing PAGE shows purified eGFP (0.8 µg) in the first lane, and an aliquot of each lysate (36 µg of total protein) at indicated time point.

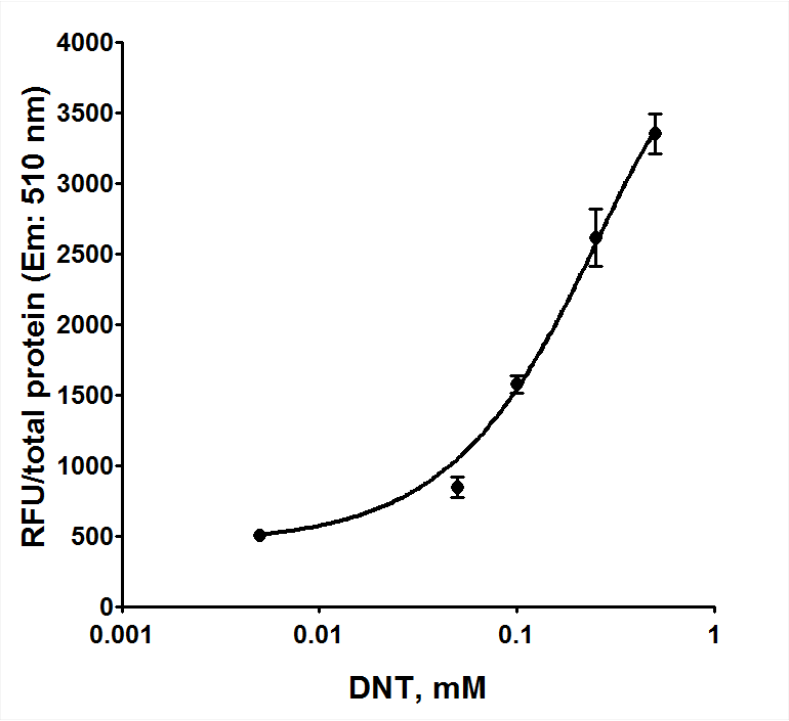

Figure 5. Dose-response graph showing fluorescence of cell lysates 6 hours after activation of riboswitch with DNT concentrations ranging from 0.005 mM to 0.5 mM

To clarify the behavior of the developed riboswitch, we investigated the switching mechanism. Relying on examination of the nucleotide sequences of different riboswitch clones (Table SI.1), we assumed that the RBS and the nucleotide sequence neighboring the RBS is involved in hybridization with the aptamer domain in the absence of analyte, resulting in translational repression of downstream gene expression. Analyte binding changes the conformation of the aptamer domain leading to unpairing of the RBS, and making the RBS sequence accessible to the ribosome. The translational regulation mechanism for synthetic riboswitches was previously identified by Gallivan and co-workers[21, 26, 27] and Yokobayashi and co-workers[28, 29].

Mfold[22] software predicted two possible low energy secondary structures for the DNT riboswitch in "OFF" state with the energies of -28.30 kcal/mol and -28.60 kcal/mol (see Figures 2 and 6). The two conformations share a common secondary structure for bases A23-U88. In the "OFF1"

configuration only two bases of RBS are involved in pairing with the aptamer domain, which could cause the fluorescence background in the "OFF" state due to riboswitch "leakage". Conversely, in the "OFF2" conformation four of the five RBS bases are involved into pairing with aptamer bases, which would lead to lower background fluorescence. In the presence of DNT molecules, the aptamer domain of the riboswitch (colored in green on Figure 6) changes its conformation and binds the ligand. The expression platform becomes less paired and the RBS is now available for ribosome binding, resulting in translation of TEV protease and increase in fluorescent signal.

To investigate the DNT-free (riboswitch in "OFF" state) and DNT-bound (riboswitch in "ON" state) structures predicted by Mfold, we performed *in vitro* enzymatic probing. *In vitro* transcribed riboswitch mRNA sequence (114 nucleotides) was treated with RNase A, which cleaves single-stranded RNA at the 3′ end of pyrimidine residues, or RNase T1, which cleaves single-stranded RNA at 3′ end of guanosine residues. The RNA fragments were separated and analysed using a 2100 Bio-Analyzer (Agilent). The experimentally observed cleavage sites and the results of enzymatic probing with RNases A and T1 are shown in Supplemental Figure SI.5, Supplemental Table SI.2, and Supplemental Figure SI.6, Supplemental Table SI.3, respectively. First, we focused on an analysis of the structure of the DNT-free (riboswitch in "OFF" state)

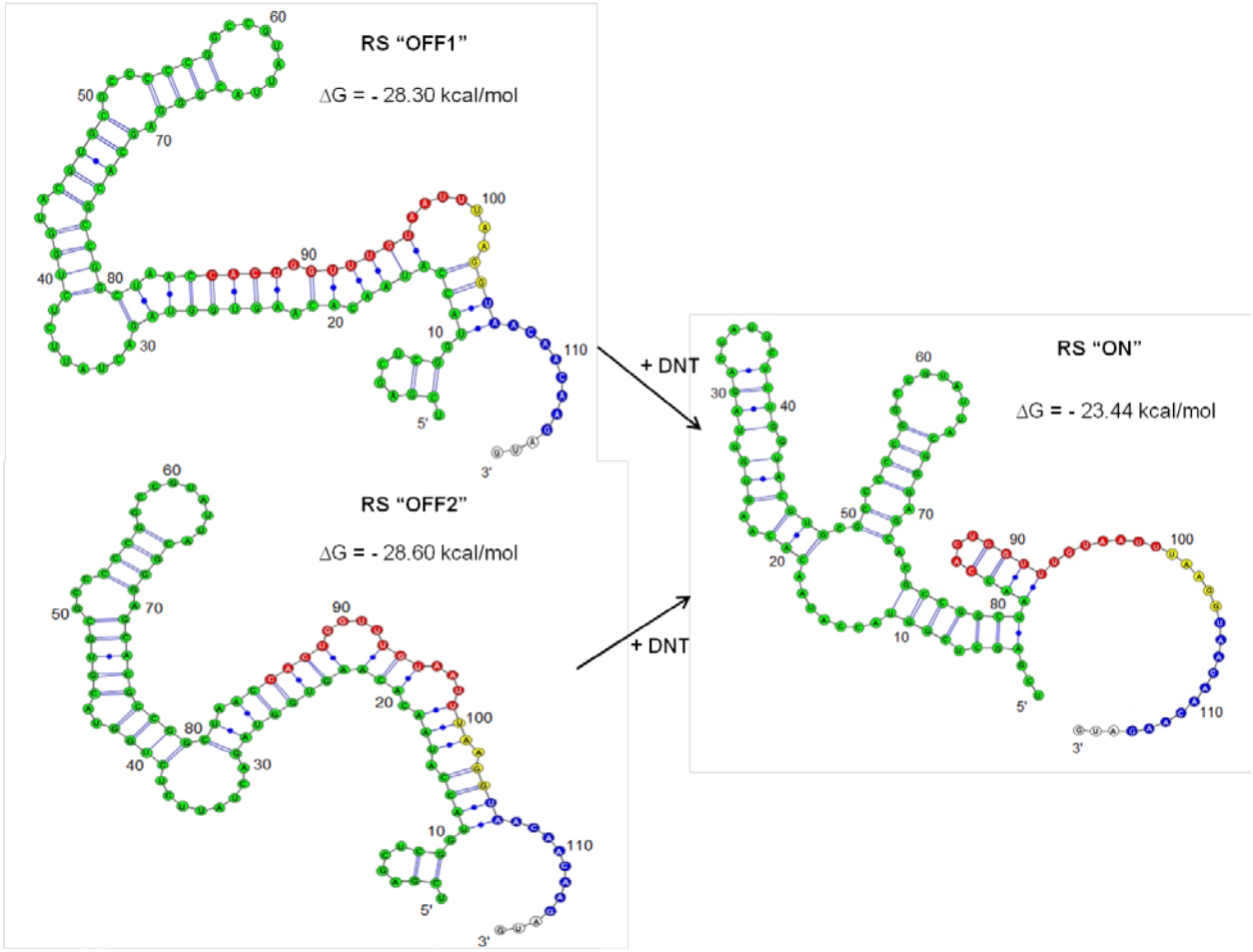

Figure 6. Predicted secondary structure of the DNT 2A-2 riboswitch in the "OFF" and "ON" states. *Green = aptamer; Red = expression platform; Yellow = RBS; White = Start Codon (AUG). There are two conformation of riboswitch in the "OFF" state with difference in energy of 0.3 kcal/mol.*

conformation. The presence of a band (band 8 on a gel in Figure SI.5D) corresponding to cleavage with RNase A at U98, U99, and U100 (Table SI.2), is more supportive of riboswitch in "OFF1" conformation, in which the indicated nucleotides are located within an unstructured loop. The cleavage with RNase T1 observed at G94 is also more indicative of riboswitch "OFF1" conformation. However, time-dependent decrease in the fluorescence background of riboswitch "OFF" state in cell-based experiments (Figure 3) could be explained by the formation of more thermodynamically stable structure of riboswitch "OFF2" conformation. Recently, Yokobayashi and co-workers showed that the thiamine pyrophosphate (TPP) sensitive riboswitch in its "OFF" state adopts two distinct structures; and

both structures contribute to the observed gene regulation by TPP riboswitch[29]. Further mutational analysis of DNT riboswitch and in vivo experiments will clarify the importance of two possible riboswitch "OFF" structures for the function of the riboswitch.

Structural analysis of the riboswitch in the presence of DNT (RS "ON") showed that the most conspicuous difference between cleavage patterns of riboswitch "ON" and riboswitch "OFF" structures occurs near the start codon (Figure SI.6 and Table SI.3). Appearance of a stronger band around G103-G104 in RNase T1 digestion (band 12 on a gel in Figure SI.6D) indicates that the ribosome binding site becomes more susceptible to cleavage in the presence of DNT. The structural predictions and experimental results support the conclusion that availability of the ribosome binding site, as a result of conformational changes, regulates translation of downstream genes in this riboswitch.

4.0 CONCLUSION

We present a design strategy for developing a ligand-inducible translational regulation system in *E. coli* cells. An aptamer selected to bind TNT molecules[11] was linked with a PCR-generated expression platform library placed upstream of the gene encoding Tobacco Etch Virus protease. Introduction of DNT turns the riboswitch "ON", producing TEV protease, which cleaves a link between the enhanced green fluorescent protein and a non-fluorescent mutant yellow fluorescent protein resulting in increased fluorescence. The selected riboswitch exhibited a 10-fold increase in fluorescence in the presence of 0.5 mM DNT compared to the system without target.

We applied enzymatic probing analysis and secondary structure analysis using Mfold to study the conformational change of the riboswitch in the presence and absence of DNT molecules. The conformational change that occurs in the presence of DNT makes the RBS available for binding, thereby permitting initiation of RNA translation and production of TEV protease. Analysis of the riboswitch in

the absence of DNT showed the existence of two distinct conformations in the "OFF" state with very close folding free energy. Similarly, two "OFF" state conformations were recently observed in the synthetic thiamine pyrophosphate riboswitch[29], which indicates both the complex nature and common structural properties of riboswitches.

Riboswitch-enabled cells are a promising environmental sensor for small toxic explosive molecule detection.

5.0 ABBREVIATIONS

DMSO, dimethyl sulfoxide;

DNT, 2,4-Dinitrotoluene;

eGFP, enhanced green fluorescent protein;

FRET, fluorescence resonance energy transfer;

nt, nucleotide;

RBS, ribosome binding site;

REACh, resonance energy accepting chromoprotein;

RNA, ribonucleic acid;

SELEX, Systematic Evolution of Ligands by EXponential Enrichment;

TEV, Tobacco Etch Virus;

TNT, 2,4,6-Trinitrotoluene.

6.0 SUPPORTING INFORMATION

6.1 Plasmid constructions

Plasmid manipulations were performed using chemically competent MAX Efficiency DH5α *E. coli* cells.

Plasmid pHWG640:eGFP-TL-REAChHis. The coding sequence of YFP was amplified from pcDNA6.2/C-YFP-DEST (Invitrogen, Carlsbad, CA) using forward (5´-CGTCATATGGTGAGCAAGGGCGAGGAG-3´) and reverse (5´-CGTAAGCTTTTAATGGTGATGGTGATGGTGCTTGTACAGCTCGTCC-3´) primers. The PCR product was digested with *Nde*I and *Hind*III and cloned into the same sites of pET21a(+) (Novagen). Sequential site-directed mutagenesis of YFP was performed with the QuikChange II Site-Directed Mutagenesis kit (Stratagene). The coding sequence of eGFP was amplified from pIVEX2.3d-eGFP using forward (5´-CGTCATATGGTGAGCAAGGGCGAGGAG-3´) and reverse (5´-CGTGGATCCGGCCTTCTTGTACAGGCTCTTGTACAGCTCGTC-3´) primers. REACh1 was amplified using forward (5´-GTGGATCCGAAAACCTGTACTTCCAGAGCGGCACCGTGAGCAAGGGCGAA-3´) and reverse (5´-CGTAAGCTTTTAATGGTGATGGTGATGGTGCTTGTACAGCTCGTCC-3´) primers. The PCR products amplified from eGFP and REACh1 were then digested with *Nde*I-*BamH*I and *BamH*I-*Hind*III, respectively, gel purified and three-way ligated into the *Nde*I-*Hind*III sites of *E. coli* expression vector pHWG640 to yield the pHWG640:eGFP-TL-REACh1 plasmid. This method of construction introduces 17 amino acid linker peptide (SLYKKAGSENLYFQSGT), which joins the C-terminus of eGFP to the N-terminus of REACh, and also places a 6XHis-tag at the N-terminus of the REACh. The linker contains a TEV protease cleavage site (underlined) and flanking spacer arms to increase TEV protease accessibility.

Plasmid pSAL:TEVHis. TEV protease coding sequence was amplified using forward (5´-CGTGGTACCAGACAACAAGATGGGAGAAAGTCTG-3´) and reverse (5´-CGTAAGCTTTTAATGGTGATGGTGATGGTGTTGCGAGTACACCAATTC-3´) primers. Purified PCR products were digested with *Kpn*I and *Hind*III, gel purified and cloned into *Kpn*I and

*Hind*III sites of bacterial expression vector pSAL to yield the pSAL:TEVHis plasmid. Expression of this plasmid in *E. coli* provides the "positive" control.

Plasmid pSAL:TNTaptTEVHis. 2,4,6-trinitrotoluene aptamer sequence upstream of TEV protease coding sequence was amplified from pJ201:26978-TNT_aptamer_TEV (DNA2.0, Menlo Park, CA) using forward (5´- CGTACCGGTTCGAGCTCGGTACCATAACACAAGTG -3´) and reverse (5´- CGTGCTCAGCTTAATGGTGATGGTGATGGTGTTGCGAGTAC -3´) primers. Purified PCR products were digested with *Age*I and *Blp*I, gel purified and cloned into *Age*I and *Blp*I sites of bacterial expression vector pSAL to yield the pSAL:TNTaptTEVHis plasmid.

Plasmid pSAL:RS2A-2TEVC151A. (C151A mutation in TEV protease sequence). The mutation C151A that yields inactive TEV protease was prepared using the QuikChange II Site-Directed Mutagenesis kit (Stratagene) using pSAL:RSTEV as a template and forward (5´- AACCAAGGATGGGCAGGCTGGCAGTCCATTAGTATC-3´) and reverse (5´- GATACTAATGGACTGCCAGCCTGCCCATCCTTGGTT-3´) primers.

PCR primer sequences for generation of riboswitch library.

Forward Primer: 5′- NNNNNNNNNNNNNNNTAAGGTAACAACAAGATGGGAGAAAGTC -3′

Reverse Primer: 5′- NNNNNNNNNNNNNNNCCGTTAGCCGGCGTGCTCCCGTAATACG -3′

6.2 Growth curves of *E. coli* TOP10 cells

Three colonies of *E. coli* TOP10 cells harboring pHWG640:eGFP-TL-ReachHis and pSAL:TEVHis from LB/agar plate containing ampicillin (100 µg/mL) and chloramphenicol (25 µg/mL) were grown overnight at 37ºC with shaking in culture tubes containing LB media (5 mL) supplemented with ampicillin (100 µg/mL) and chloramphenicol (25 µg/mL). 20 µL of the overnight culture was used to inoculate 1 mL of LB media in 24-well plate (Becton Dickinson) supplemented with ampicillin (100 µg/mL), chloramphenicol (25 µg/mL), and appropriate concentration of 2,4-dinitroroluene. Plates were shaken at 215 rpm at 37ºC. The OD_{600} readings for each well were recorded using plate-reading spectrophotometer (Molecular Devices Spectra

Max M5) every hour for seven hours, along with a final 24-hour reading. All growth studies were conducted in triplicate, and data are presented as the mean ± s.e.m.

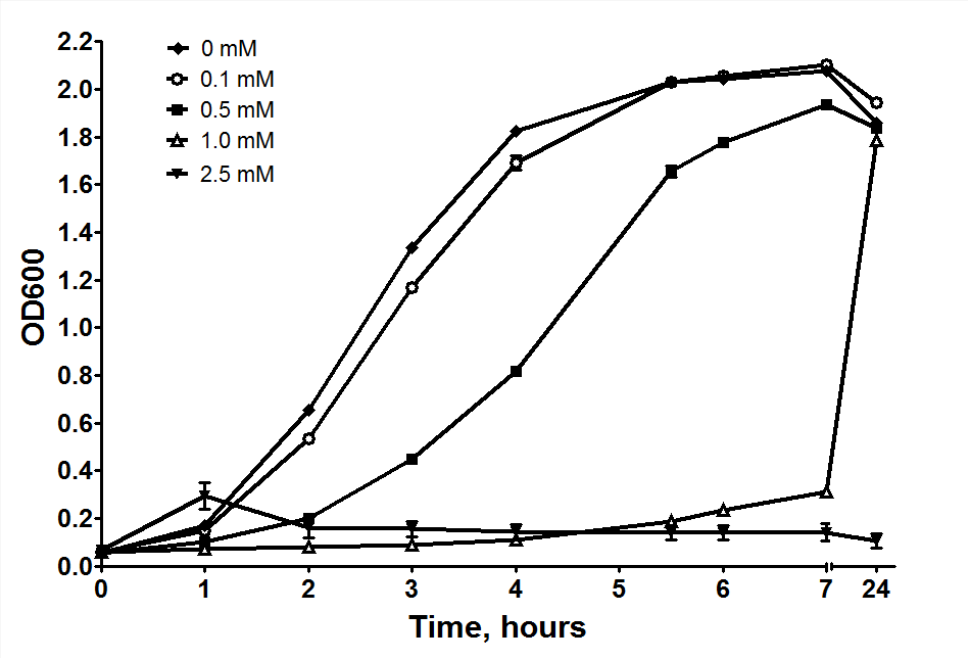

Figure SI.1. Growth curves of *E. coli* cells in the presence of varying concentrations of 2,4-dinitrotoluene

Table SI.1. Top five riboswitch clones and their expression platform sequences. Randomized inserts are underlined

Clone	Activation Ratio	Sequence
2A-2	9.8	CACTGGTTTGTAATTTAAGGTAACAACAAG
1B-7	3.3	GATAATGGCAAGACACAGTATGTGGGGGGGTTAGGTAACAACAAG
1A-3	3.2	CTCTGAAGGTTGAGGGATAAGGTAACAACAAG
1B-10	3.2	TGATGGAACGACTACTGTCTCAAGTAATGTAAGGTAACAACAAG
1C-8	3.2	GAACTCAATGGTTTGTGTAATTGGTAAGGTAACAACAAG

.

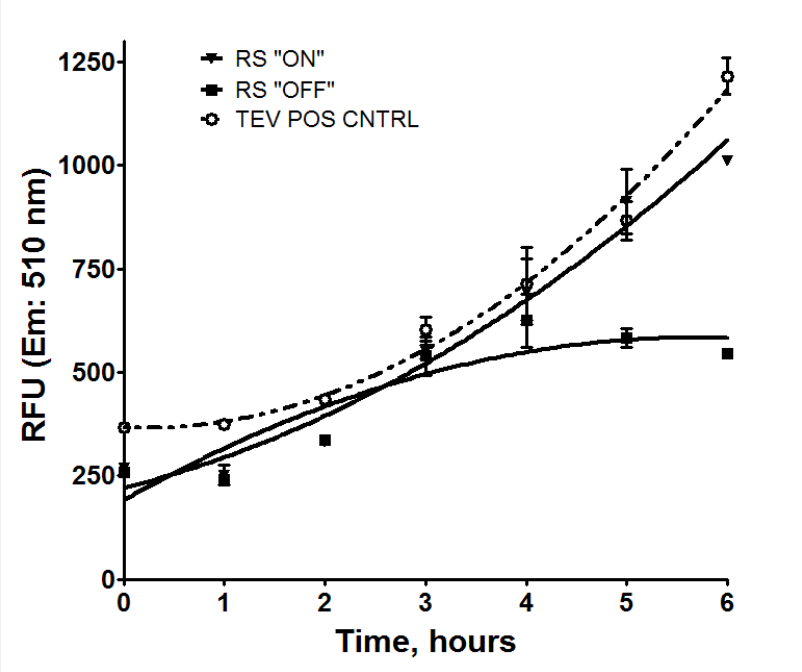

Figure SI.2. Changes in the fluorescence intensity of cell cultures in the presence of 0.5 mM DNT over time.

The fluorescence intensity of cells expressing pHWG640:eGFP-TL-REACh and one of the following constructs: pSAL:TEV (TEV POS CNTRL) (white circles), pSAL:2A-2TEV in the presence of DNT (RS "ON") (inverted black triangles), or pSAL:2A-2TEV (RS "OFF") (black squares), was monitored at 510 nm upon excitation at 457 nm. 0.5 mM DNT was added at time 0, and samples were collected at indicated time points. RFU represents the relative fluorescence intensity units.

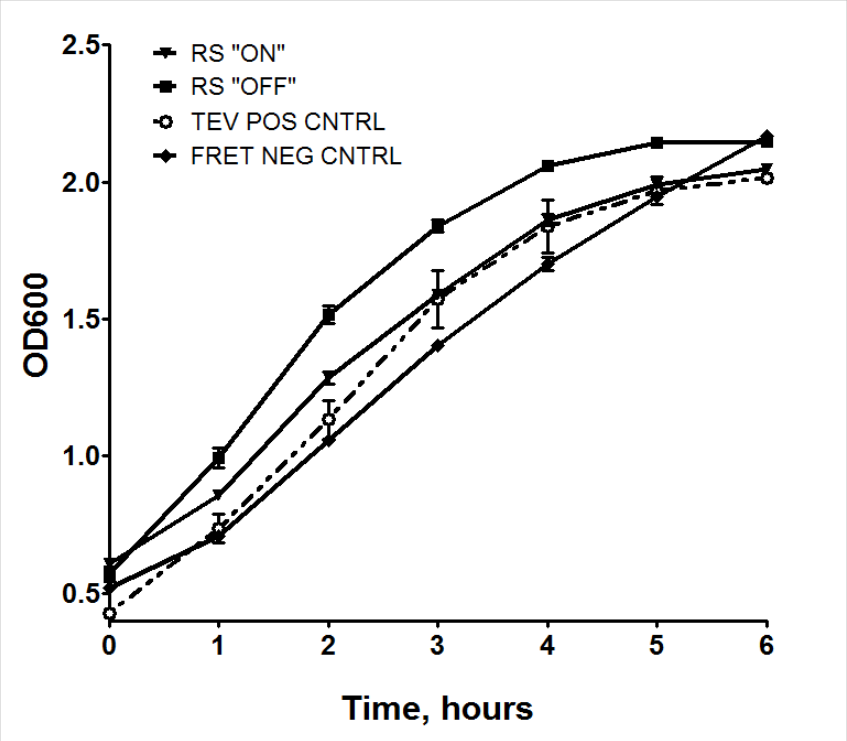

Figure SI.3. Growth curves of TOP10 *E. coli* cells without or in the presence of 0.5 mM DNT. *TOP10 E. coli cells harboring either the positive control (pHWG640:eGFP-TL-REACh1His and pSAL:TEVHis), riboswitch (pHWG640:eGFP-TL-REACh1His and pSAL:2A-2TEVHis), or negative control (pHWG640:eGFP-TL-REACh1His and pSAL:RSTEVC151A) were grown to mid-log phase at 37˚C and then induced with rhamnose. DNT was added (30 min after rhamnose induction) to the "on" state of riboswitch, which is indicated by time 0 on the graph.*

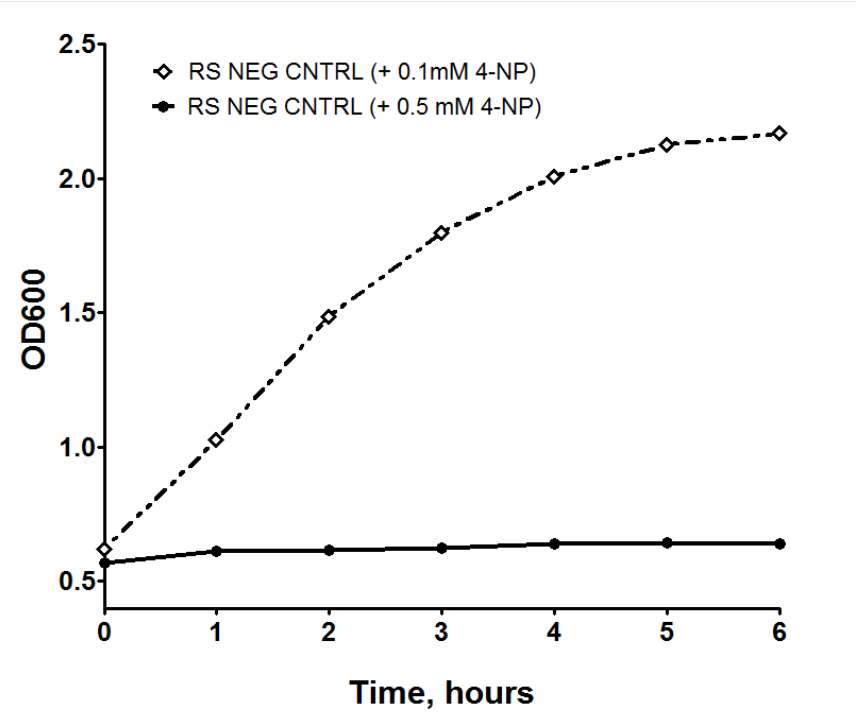

Figure SI.4. Growth of TOP10 *E. coli* cells in the presence of different concentrations of 4-nitrophenol.

TOP10 E. coli cells harboring pHWG640:eGFP-TL-REACh and pSAL:2A-2TEV (RS NEG CNTRL) were grown to mid-log phase at 37˚C and then induced with rhamnose. 0.1 mM or 0.5 mM 4-nitrophenol (4-NP) was added after 30 min, indicated by time 0 on the graph.

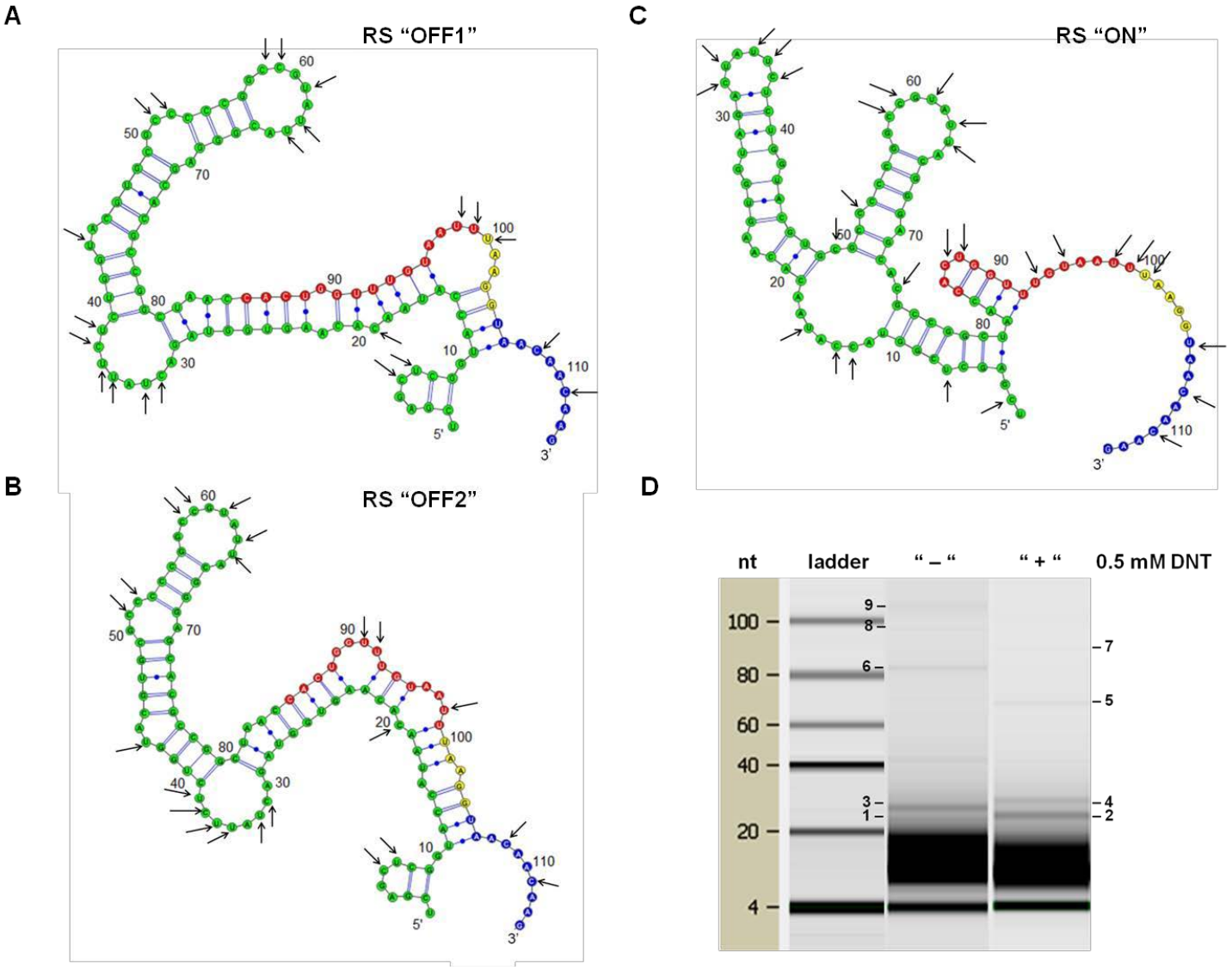

Figure SI.5. Enzymatic probing analysis of 2A-2 DNT-responsive riboswitch with RNase A
In vitro transcribed non-labeled mRNA riboswitch sequence (114 nucleotides) was digested by RNase A with or without 0.5 mM DNT. RNase A cleaves single-stranded RNA at the 3´ end of pyrimidine residues. The observed cleavage sites were schematically mapped onto the mFold-predicted analyte-free (RS "OFF1" and RS "OFF2") (A, B) and analyte-bound (RS "ON") (C) structures. The cleaved RNA was analyzed using a 2100 BioAnalyzer (Agilent). The visualization of obtained RNA fragments was performed using a fluorescent dye that binds to nucleic acid and was provided with Small RNA Kit from Agilent. The resulting data were translated into a gel-like image for ease of analysis (D).

Table SI.2. Structural analysis of 2A-2 riboswitch sequence with RNase A.

Band	RNA fragments corresponding to RS "OFF 1" state	RNA fragments corresponding to RS "OFF 2" state	RNA fragments corresponding to RS "ON" state
1, 2	U7-C32; U33-C58; U36-U61; U38-U63; C6-C32; U7-U33; C32-C58; U33-C59; U35-U61; C37-U63; U38-U64; C6-U33; C32-C59; U36-U63; C37-U64; U7-U35; U33-U61; U35-U63; U36-U64; C6-U35; U7-U36; C32-U61; U35-U64	U7-C32; U33-C58; U36-U61; U38-U63; C6-C32; U7-U33; C32-C58; U33-C59; U35-U61; C37-U63; U38-U64; C6-U33; C32-C59; U36-U63; C37-U64; U7-U35; U33-U61; U35-U63; U36-U64; **U63-U91; U64-U92**; C6-U35; U7-U36; C32-U61; U35-U64; **U63-U92**	C13-U36; C14-C37; U35-C58; U36-C59; U64-C87; C13-C37; U35-C59; C37-U61; U63-C87; U64-U88; C74-U98; U7-C32; U33-C58; U36-U61; C49-C74; U63-U88; C74-U99; U7-U33; C32-C58; U33-C59; U35-U61; C37-U63; U61-C87; C74-U100
3, 4	C19-U61; **C58-U100**; U43; U7-C51; C19-U63; U64-C108; C6-C51; U7-C52; C19-U64; U63-C108; C6-C52; C52-U98	C19-U61; U43; U7-C51; C19-U63; U64-C108; C6-C51; U7-C52; C19-U64; U63-C108; C6-C52; C52-U98	U33; C2-U35; U16-C49; C2-U36; C59-U93; U61-U95; U64-U98; C74-C108; U35; C2-C37; C14-C49; C52-C87; C58-U93; U63-U98; U64-U99
5, 6	C19-U100; U33 (3'-end); C32 (3'-end)	U33 (3'-end); C32 (3'-end)	U35-U105; U16-C87; C37-C108; C2-C74; U16-U88; U33-U105; U36-C108; C14-C87; C32-U105; U35-C108
7, 8	U98; U99; U100	U98	U16-U105; C2-U93; U7-U98; C14-U105; U7-U99; C13-U105; U16-C108
9	U7 (3'-end); C108; C6 (3'-end); C111	U7 (3'-end); C108; C6 (3'-end); C111	

Each band from the gel-like image shown in Figure SI.5D can be identified as a possible RNA fragment obtained after cleavage by RNase A of indicated riboswitch conformations. RNase A cleaves single-stranded RNA at the 3´ end of pyrimidine residues. The oligonucleotide fragments anticipated for the riboswitch "OFF" structures, RS "OFF1" or RS"OFF2", are in bold; the fragments anticipated for the riboswitch "ON" state structure are underlined.

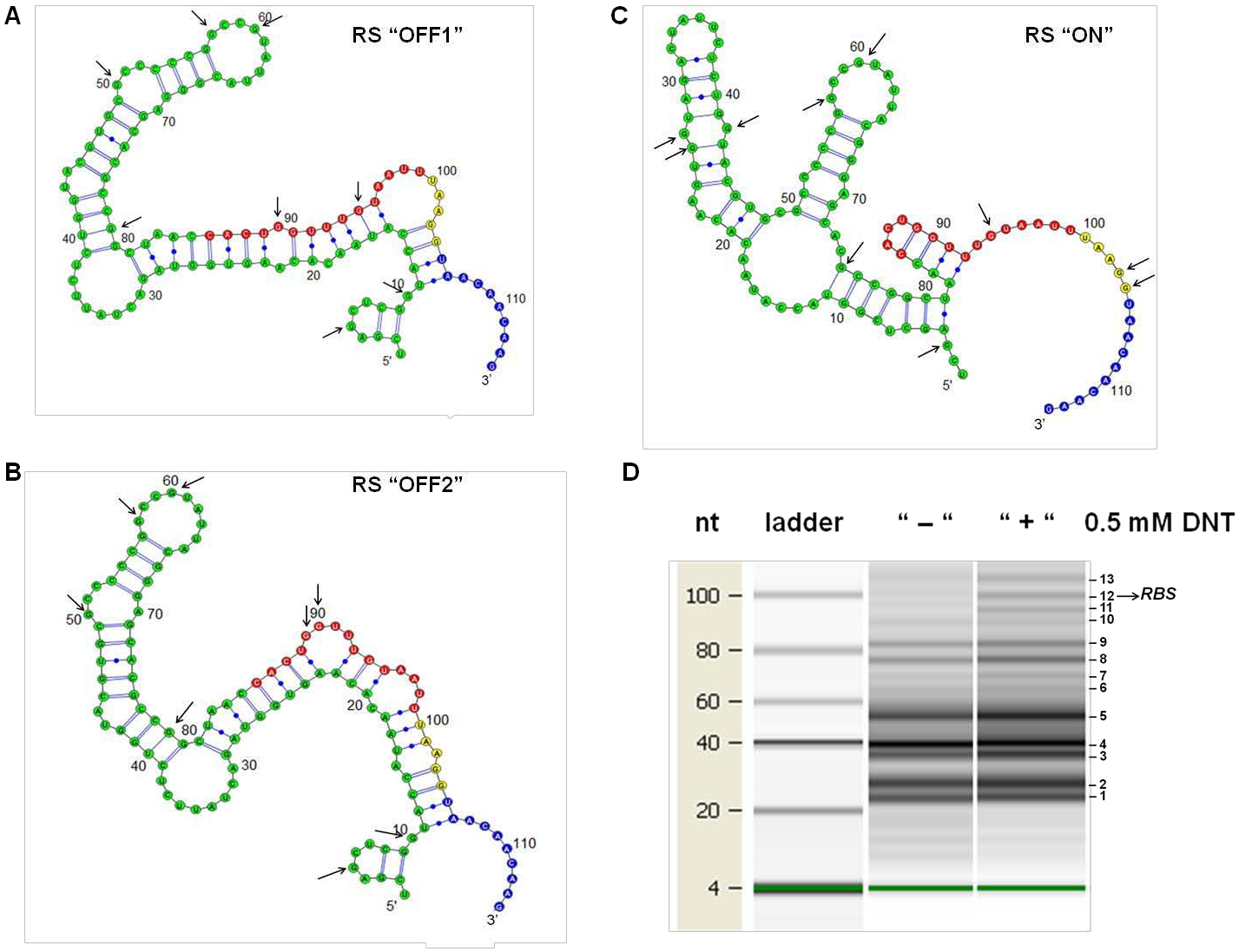

Figure SI.6. Enzymatic probing analysis of 2A-2 DNT-responsive riboswitch with RNase T1

In vitro transcribed non-labeled mRNA riboswitch sequence (114 nucleotides) was digested by RNase T1 with or without 0.5 mM DNT. RNase T1 cleaves single-stranded RNA at 3´ end of guanosine residues. The observed cleavage sites were schematically mapped onto the mFold-predicted analyte-free (RS "OFF1" and RS "OFF2") (A, B) and analyte-bound (RS "ON") (C) structures. The cleaved RNA was analyzed using a 2100 BioAnalyzer (Agilent). The visualization of obtained RNA fragments was performed using a fluorescent dye that binds to nucleic acid and was provided with the Small RNA Kit from Agilent. The resulting data were translated into gel-like image for ease of analysis (D).

Table SI.3. Structural analysis of 2A-2 riboswitch sequence with RNase T1

Band	RNA fragments corresponding to RS "OFF 1" state	RNA fragments corresponding to RS "OFF 2" state	RNA fragments corresponding to RS "ON" state
1	G57-G78; G89-G114	G57-G78; **G90-G114**; G89-G114	G3-G26; G3-G27; G26
2	G50-G78; G60-G89; G57-G89	G50-G78; G60-G89; **G60-G90**; G57-G89; **G57-G90**	G27; G75-G103; G75-G104; G27-G57; G26-G57; G27-G60; G42-G75
3	**G60-G94**; G78-G114; **G57-G94**	G78-G114	G26-G60; G41-G75; G60-G94; G57-G94; G3-G41
4	G50-G89; G10-G50	G50-G89; G10-G50; **G50-G90**	G3-G42; G42; G60-G103; G60-G104
5	G50; G10-G60; G5-G57; G60-G114; G5-G60	G50; G10-G60; G5-G57; G60-G114; G5-G60	G42-G94; G41-G94; G3-G57; G60-G114; G57-G104; G27-G75; G26-G75
6	G57; G57-G114; G60; G50-G114	G57; G57-G114; G60; G50-G114	G41-G103; G42-G104; G41-G104
7	G10-G78; G5-G78	G10-G78; G5-G78	G26-G94; G3-G75; G42-G114; G41-G114
8	G78; G10-G89	G78; G10-G89	G26-G94; G3-G75; G42-G114; G41-G114
9	G5-G89; G10-G94	G10-G90; G5-G89; **G5-G90**	G26-G114; G27-G114
10	G89; **G5-G94**	G89; **G90**	G3-G94
11	**G94**		G94
12	G10-G114	G10-G114	G103; G104
13	G5-G114	G5-G114	G3-G114

Each band from the gel-like image shown in Figure SI.6D can be identified as a possible RNA fragment obtained after cleavage by RNase T1 of indicated riboswitch conformations. RNase T1 cleaves single-stranded RNA at 3´ end of guanosine residues. The oligonucleotide fragments anticipated for the riboswitch "OFF" structures, RS "OFF1" or RS"OFF2", are in bold; the fragments anticipated for riboswitch "ON" state structure are underlined.

7.0 REFERENCES

(1) Blouin, S., Mulhbacher, J., Penedo, J.C., Lafontaine D.A. *ChemBioChem.* 2009, 10, 400-416.

(2) Topp, S., and Gallivan, J.P. *ACS Chem. Bio*. 2010, 5(1), 139-148.

(3) Gu, M.B., Chang, S.T. *Biosens Bioelectron.* 2001, 16, 667-674.

(4) Gu, M.B., Choi, S.H., Kim, S.W. *J Biotechnol.* 2001, 88, 95-105.

(5) Mbenkui, F., Richaud,,C., Etienne, A.L., Schmid, R.D., Bachmann, T.T. *Appl Microbiol Biotechnol.* 2002, 60, 306-312.

(6) Premkumar, J.R., Rosen, R., Belkin, S., Lev, O. *Anal Chim Acta.* 2002, 462, 11-23.

(7) Tuerk, C. and Gold, L. *Science. 1990,* 249, 505-510.

(8) Roth, A., Breaker, R.R. *Methods in Molecular Biology*, vol. 252: Ribozymes and siRNA Protocols, 2nd ed. Humana Press, Inc.; 2004, 145-164.

(9) Suess, B., and Weigand, J.E. *RNA Biology* 2008, 5(1), 1-6.

(10) Sinha, J., Topp, S., and Galliva, J.P. *Methods in Enzymology* 2011, 497, 207-220.

(11) Ehrentreich-Förster, E., Orgel, D., Krause-Griep, A., Cech, B., Erdmann, V.A., Bier, F., Scheller, F.W., Rimmele, M. *Anal Bioanal Chem*. 2008, 391, 1793-1800.

(12) Suski, J.G., Salice, C., Houpt, J.T., Bazar, M.A., and Talent, L.G. *Environ. Toxicol. Chem.* 2008, 27, 352-359.

(13) Spanggord, R.J., Gibson, B.W., Keck, R.G., and Thomas, D.W. *Environ. Sci. Technol.* 1982, 16(4), 229-232.

(14) Yang, H., Zhao, J.-S., and Hawari, J. *Journal of Applied Microbiology* 2009, 107, 1799-1808.

(15) Xu, J., and Jing, N. *J. Hazard Mater.* 2012, 203-204, 299-307.

(16) Tyson, C.A., Dilley, J.V., Sasmore, D.P., Spanggord, R.J., Newell, G.W., Dacre, J.C. *J. Toxicol. Environ. Health* 1982, 9(4), 545-564.

(17) Lent E.M., Crouse, L.C., Quinn, M.J. Jr, Wallace, S.M. *Int. J. Toxicol.* 2012, 31(2), 143-157.

(18) Klaassen, C.D., editor. Casarett & Doull's Toxicology. 6th ed. New York: McGraw-Hill; 2001, 1236 p.

(19) Ganesan, S., Ameer-beg, S.M., Ng, T.T., Vojnovic, B., Wouters, F.S. *Proc. Nat. Acad. Sci. U.S.A.* 2006, 103, 4089-4094.

(20) Harbaugh, S., Kelley-Loughnane, N., Davidson, M., Narayanan, L., Trott, S., Chushak, Y.G., Stone, M.O. *Biomacromol. 2009*, 10, 1055–1060.

(21) Lynch, S.A., Gallivan, J.P. *Nucleic Acids Res.* 2009, 37(1), 184-192.

(22) Zuker, M. *Nucleic Acids Res.* 2003, 31(13), 3406-3415.

(23) Rickert, D.E., Butterworth, B.E., and Popp, J.A. *Crit. Rev. Toxicol*. 1984, 13, 217-233.

(24) Banerjee, H.N., Verma, M., Hou, L-H., Ashraf, M., and Dutta, S.K. *Yale Journal of Biology and Medicine*, 1999, 72, 1-4.

(25) Hall, B, Hesselberth, J.R., Ellington, A.D. *Biosens. Bioelectron*. (2007), 22: 1939–1947.

(26) Lynch, S.A., Desai, S.K., Sajja, H.K., and Gallivan, J.P. *Chem. Biol,*. 2007, 14(2), 173-84.

(27) Sinha, J., Reyes, S.J., and Gallivan, J.P. Nat. Chem. Biol., 2010, 6(6), 464-470.

(28) Nomura, Y., and Yokobayashi, Y. *J. Am. Chem. Soc*., 2007, 129, 13814-13815.

(29) Muranaka, N., Sharma, V., and Yokobayashi, Y. *Nucleosides, Nucleotides and Nucleic Acids*, 2011, 30, 696-705.

8.0 SUMMARY GRAPHIC